RESEARCH

A comprehensive prognostic and immunological implications of PFKP in pan-cancer

Xiaodong Ling[1], Luquan Zhang[1], Chengyuan Fang[1], Hao Liang[1] and Jianqun Ma[1*]

Abstract

Background Phosphofructokinase P (PFKP) is a key rate-limiting enzyme in glycolysis, playing a crucial role in various pathophysiological processes. However, its specific function in tumors remains unclear. This study aims to evaluate the expression and specific role of PFKP across multiple tumor types (Pan-cancer) and to explore its potential clinical significance as a therapeutic target in cancer treatment.

Methods We analyzed the expression of PFKP, immune cell infiltration, and patient prognosis across various cancers using data from the Cancer Genome Atlas (TCGA) and Gene Expression Omnibus (GEO) databases. Additionally, we conducted a series of experiments in lung cancer cells, including Western blot, CCK-8 assay, colony formation assay, transwell migration assay, scratch wound healing assay, LDH release assay, and flow cytometry, to evaluate the impact of PFKP on tumor cells.

Results PFKP was found to be highly expressed in most cancers and identified as a prognostic risk factor. Elevated PFKP expression is associated with poorer clinical outcomes, particularly in lung adenocarcinoma (LUAD). Receiver operating characteristic (ROC) curve analysis indicated that PFKP can effectively differentiate between cancerous and normal tissues. The expression of PFKP in most tumors showed significant correlations with tumor mutational burden (TMB), microsatellite instability (MSI), immune score, and immune cell infiltration. In vitro experiments demonstrated that PFKP overexpression promotes lung cancer cell proliferation and migration while inhibiting apoptosis, whereas PFKP deficiency results in the opposite effects.

Conclusion PFKP acts as an oncogene involved in tumorigenesis and may influence the immune microenvironment within the tumor. Our findings suggest that PFKP could serve as a potential biomarker for predicting prognosis and the efficacy of immunotherapy in tumors.

Keywords PFKP, Pan-cancer, LUAD, Prognosis prediction, Immune analysis

*Correspondence:
Jianqun Ma
jianqunma@hrbmu.edu.cn
[1]Department of Thoracic Surgery, Harbin Medical University Cancer
Hospital, 150 Haping Road, Harbin, Heilongjiang 150040, China

Introduction

Cancer remains one of the leading causes of death worldwide, with high incidence and mortality rates, making it a critical public health concern. Traditional cancer treatments, such as surgery, radiation therapy, and chemotherapy, have been supplemented in recent years by rapid advancements in immunotherapy and molecular targeted therapies. Despite some progress in comprehensive cancer treatment, tumor progression remains a significant challenge, and the average survival rates for cancer patients are still low. Therefore, it is crucial to thoroughly analyze the genomic characteristics of tumors to identify effective therapeutic targets and strategies, which are essential for improving treatment outcomes and patient prognosis.

The PFKP gene is situated on the diminutive extremity of chromosome 10 within the human genome [4]. PFKP exhibits 8 diverse transcript variants, and isoform 1 emerges as the most protracted of these, spanning a length of 784 amino acids. The regulation of PFKP gene expression is intricately entwined with the process of glycolysis. Phosphofructokinase (PFK) is a pivotal rate-limiting enzyme in glycolysis, which accelerates the consumption of glucose [5]. PFK encompasses three subtypes: PFKP (platelet), PFKM (muscle), and PFKL (liver). Moreover, all subtypes are found in other tissues as well [6]. PFKP exhibits expression in various cell types, gaining recognition for its crucial role in different types of cancers, including non-small cell lung cancer and breast cancer [7, 8]. Research indicates that the downregulation of PFKP reduces glucose uptake rate, thereby inhibiting the growth of lung cancer cells. Additionally, PFKP regulates non-glycolytic functions related to metabolic stress induced by glucose deprivation in NSCLC cells through AMPK-mediated regulation of long-chain fatty acid oxidation. Thus, PFKP may serve as a prognostic indicator for lung cancer, and its regulatory role in glycolysis could be a potential therapeutic target for the disease. Gao et al. reported the involvement of Nuclear PFKP in promoting CXCR4-dependent infiltration by T-cell acute lymphoblastic leukemia. However, the critical role of PFKP in most tumors remains unexplored. The advent of next-generation sequencing (NGS) technology and in-depth exploration of cancer genome atlas (TCGA) datasets gradually reveal genomic and transcriptomic data of common tumors to researchers. Therefore, this is an optimal approach for scrutinizing and revealing the prospective prognostic and predictive significance of biomarkers through Pan-cancer analysis in the realm of precision medicine.

In this study, we identified significant differences in the expression of PFKP by analyzing differentially expressed genes between tumor cells of epithelial origin and normal cells. Furthermore, we explored the expression of PFKP in Pan-cancer and its clinical relevance. Additionally, we analyzed the relationship between PFKP expression and tumor mutation burden, microsatellite instability, and immune phenotype scores. Lastly, we determined the status of immune infiltration and immunotherapy sensitivity in different subgroups.

Materials and methods

Data acquisition and processing

We downloaded the RNA-Seq expression data of 33 different tumors from the TCGA database. We determined the expression levels of PFKP in 33 types of tumors. Additionally, we used a web-based analysis tool, the Gene Expression Profiling Interactive Analysis (GEPIA) [9], to visualize the PFKP expression levels in different stages of all tumors. Then, we explored the protein expression level of PFKP between normal and tumor tissues through the University of ALabama at Birmingham CANcer data analysis Portal (UALCAN) [10]. To verify the expression of PFKP between the tumor and normal cells in LUAD, the single-cell RNA transcriptome data of GSE117570 were downloaded from the GEO database.

Survival analysis

Patients were divided into high- and low-expression groups using the minimum *P*-value method. Cox regression analysis for TCGA datasets was performed using RStudio software with the "survival" and "forestplot" packages to investigate the correlation between PFKP expression and cancer prognosis, including overall survival (OS), disease-specific survival (DSS), disease-free interval (DFI), and progression-free interval (PFI). We calculated the log-rank *P*-value and hazard ratio (HR) with 95% confidence intervals (95% CI) via the "survival" package and utilized the "forestplot" package to visualize the survival analysis [11]. We also implemented the Kaplan-Meier survival analysis to estimate the clinical outcomes of patients with PFKP^{low} or PFKP^{high} tumors by executing the "survival" and "survminer" R packages. For grouping, we employed the minimum P-value approach to identify the optimal cutoff for the continuous variable X. First, X was sorted, and potential cutoff points were assessed, dividing the data into two groups. The P-values for each cutoff were calculated using the Log-rank test, with the smallest P-value determining the optimal cutoff. To address multiple testing issues, Bonferroni correction was applied to adjust the P-values, ensuring robust results. The final optimal cutoff was then used in subsequent survival analyses to evaluate the impact of X on outcomes.

Correlation analysis of PFKP with TMB, MSI, immunophenotype scores, and tumor immune microenvironment

The genome alterations of PFKP included copy number amplification, deep or shallow deletion, missense mutation with uncertain significance and messenger RNA (mRNA) upregulation. Tumor mutation burden (TMB) is calculated as total somatic nonsynonymous mutation counts in coding regions. Numerous studies have explored the significance of using TMB as a biomarker for identifying patients sensitive to checkpoint inhibitors [12]. Microsatellite instability (MSI) is featured by the widespread length polymorphisms of microsatellite sequences resulting from DNA polymerase slippage [13]. The TMB and MSI scores were obtained from TCGA database and Spearman's rank method was used to determine the correlation of PFKP with TMB and MSI. The correlation results for TMB and MSI were visualized in radar maps. We also retrieved the immunophenoscore (IPS) for LUAD patients from The Cancer Immunome Atlas. The IPS is calculated based on four significant categories of tumor immunogenicity determinants, including effector cells, immunosuppressive cells, MHC molecules, and checkpoints/immunomodulators [14]. Regarding the level of immune cell infiltration, these differences were further explored using seven methods from the TIMER 2.0 website, including (TIMER [15], XCell [16], EPIC [17], QUANTISEQ [18], CIBERSORT-ABS [19], MCP counter method [20] and CIBERSORT [20]. Pearson correlation analysis was conducted to assess the correlations between risk scores and immune scores, as well as their association with immune-infiltrating cells.

We made comparisons of IPS for the PFKP^low and PFKP^high groups and subsequently evaluated their responses to anti-PD1/PDL1/PDL2 and anti-CLA4 treatments. The stromal score and immune score were compared among different groups by the ESTIMATE (Estimation of Stromal and Immune cells in Malignant Tumor tissues using Expression data) method [21].

Comprehensive analysis of single cell datasets and cell cluster annotation

The single-cell sequencing data, including BRCA (Breast Cancer), CHOL (Cholangiocarcinoma), COAD (Colon Adenocarcinoma), ESCC (Esophageal Squamous Cell Carcinoma), GIST (Gastrointestinal Stromal Tumor), LIHC (Liver Hepatocellular Carcinoma), LUNG (Lung Cancer), OVCA (Ovarian Cancer), PAAC (Pancreatic Adenocarcinoma), PDAC (Pancreatic Ductal Adenocarcinoma), PRAD (Prostate Adenocarcinoma), STAD (Stomach Adenocarcinoma), THCA (Thyroid Carcinoma), and UCEC (Uterine Corpus Endometrial Carcinoma), are derived from GSE210347, GSE145370 and GSE203612. We analyzed the scRNA-seq data using the

R package Seurat [22]. The data were normalized using the SCTransform method and integrated using the IntegrateData function. T-distributed stochastic neighbor embedding (t-SNE) and Uniform Manifold Approximation and Projection (UMAP) were applied to reduce the dimensions. The FindNeighbors and FindClusters functions were used for cell clustering analysis.

Cell culture and transfection

The six human NSCLC cell lines (H1915, A549, PC9, H460, H1650, and H1299) were obtained from Laboratory of Medical Genetics (Department of Biology, Harbin Medical University, Harbin, China). Cells were cultured in RPMI-1640 (Invitrogen Corporation, Carlsbad CA, USA) supplemented with 10% FBS (PAN-Biotech, Aidenbach Germany). Cell cultures were kept in a humidified incubator at 37℃ with 5% CO_2.

The H1299 cells were transfected with PFKP siRNA to knock down the PFKP expression according to the manufacturer's protocols. The duplex sequences of the three siRNA targeting PFKP were as follows: First, sense, 5′- GGAGCAAUUGAUACCCAAATT-3′, and antisense, 5′-UUUGGGUAUCAAUUGCUCCTT-3′; Second, sense, 5′-GCAACGUAGCUGUCAUCAATT-3′, and antisense, 5′-UUGAUGACAGCUACGUUGCTT-3′; Third, sense, 5′-CCCUCUCCAUUUGAUAGAATT-3′, and antisense, 5′-UUCUAUCAAAUGGAGAGGGTT-3′.

Western blot

Cells were lysed using RIPA buffer (Solarbio, Beijing, China). Protein samples were electrophoresed in 15% SDS-PAGE and transferred to PVDF membranes. After blocking with PBST containing 5% nonfat milk, membranes were incubated with primary antibodies against PFKP (ab119796, Abcam, UK) and GAPDH (2118 S, Cell signaling technology, USA) at 4 ℃ overnight. Then, the membranes were incubated with a secondary antibody (Beijing Zhongshan Golden Bridge Biotechnology Co. Ltd., Beijing, China) for 1 h at room temperature. Finally, the ECL (Tanon, Shanghai) detection system was used to visualize the protein bands.

Cell proliferation assay

Cells with a density of 3×10^3/ml were seeded in a 96-well plate, and cultured for 24, 48, and 72 h. the OD values were measured using Cell Counting Kit 8 (CCK-8, Elabscience, China). Subsequently, the OD values were measured at 450 nm with a microplate reader.

Colony formation assay

Cells were plated in a 12-well plate at a density of 500 cells per well. Cells grew for ten days in a 37 ℃ incubator until more than 50 cells were available for most clones. Then, cells were fixed with 4% paraformaldehyde for

Ling *et al. Cancer Cell International*   (2024) 24:310

Page 4 of 15

20 min, followed by staining with 0.2% crystalline violet solution for half an hour at room temperature and washing with PBS three times.

Wound-healing assay

For wound healing assay, a wound was generated in a 6-well plate by scratching the surface with a 1 mL pipette tip. Scratch width change was measured under a light microscope (Nikon, Tokyo, Japan) after 24 h of culture in serum-free 1640 medium.

LDH Release Assay

Cell suspensions of treated cancer cells were added to 96-well plates at a density of 1,000 to 5,000 cells per well. After cell attachment, LDH was determined at 24, 48, and 72 h using an LDH Cytotoxicity Assay Kit (C0016, Beyotime Biotechnology, China), following the manufacturer's instructions.

Apoptosis analysis

Apoptosis was detected using Annexin V-FITC Apoptosis Detection Kit (C1062M, Beyotime Biotechnology, China). Briefly, according to the manufacturer's protocol, cells were stained with FITC- and PE-conjugated antibodies and incubated in the dark for 20 min. Quantification of apoptotic cells was then performed using a FACS Calibur flow cytometer.

Migration assay

Serum-free tumor cell suspensions were added to the upper chambers of Transwell inserts at a density of 5×10^4 cells per well, while the lower chambers were filled with culture medium containing 10% FBS. After 18 h, the cells were fixed, stained, and photographed under a microscope.

Statistical analysis

All bioinformatic analyses were carried out with the R software version 4.1.3. The survival curve was plotted by Kaplan-Meier survival curve. The Wilcoxon test was applied in analyzing differences between clinical feature distribution, immune infiltration, and therapy response. Double-tailed $p < 0.05$ was considered statistically significant.

Results

Expression level of PFKP in pan-cancer single-cell sequencing (scRNA-seq)

The flowchart of this study was shown in Fig. 1. We first collected pan-cancer single-cell datasets from 14 types of tumors, including BRCA (Breast Cancer), CHOL (Cholangiocarcinoma), COAD (Colon Adenocarcinoma), ESCC (Esophageal Squamous Cell Carcinoma), GIST (Gastrointestinal Stromal Tumor), LIHC (Liver Hepatocellular Carcinoma), LUNG (Lung Cancer), OVCA (Ovarian Cancer), PAAC (Pancreatic Adenocarcinoma), PDAC (Pancreatic Ductal Adenocarcinoma), PRAD (Prostate Adenocarcinoma), STAD (Stomach Adenocarcinoma), THCA (Thyroid Carcinoma), and UCEC (Uterine Corpus Endometrial Carcinoma), obtaining a total of 943,839 cells from scRNA-seq data. After log normalization and dimensionality reduction, these cells were further annotated into six cell types based on the expression of cell markers (Fig. 2A). The bubble plot of marker genes is shown in Fig. 2B. Next, we validated the accuracy of cell subtype annotations by examining the UMAP expression plots of marker genes across different cell clusters (Fig. 2C-J). Finally, we analyzed the expression of PFKP across various cell subtypes in the pan-cancer single-cell data (Fig. 2K). The results show that PFKP is highly expressed in tumor cells, particularly in LUNG, OVCA, and PAAC, suggesting a potential link between PFKP and tumorigenesis.
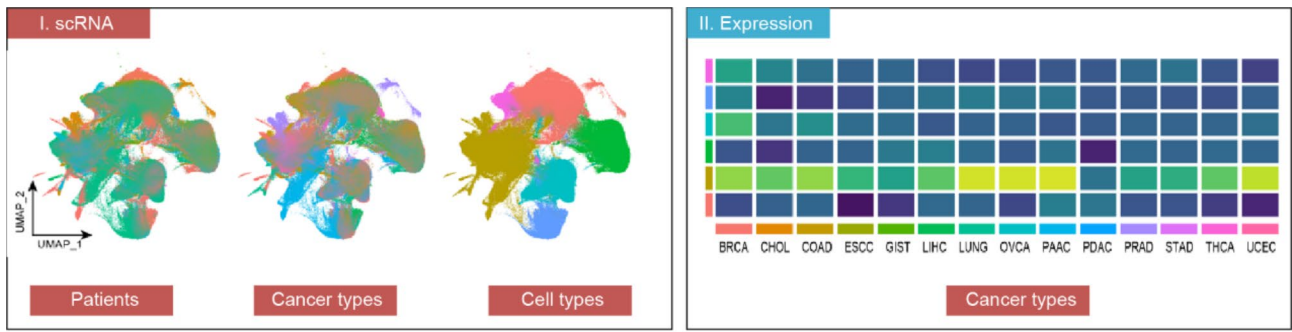
Expression levels of PFKP in pan-cancer

We first compared PFKP expression between tumor and normal tissues from the TCGA database. The results showed that the expression level of PFKP in the tumor tissues of CHOL, COAD, ESCA, HNSC, KIRC, KIRP, LIHC, LUAD, LUSC, PCPG, STAD, and UCEC is much higher than the corresponding normal tissues (Fig. 3A). In paired samples, PFKP expression was significantly elevated in multiple cancer types, including CHOL, COAD, HNSC, KIRC, KIRP, LIHC, LUAD, LUSC, and STAD (Fig. 3B). Furthermore, PFKP expression levels increased with tumor progression in ACC, KIRC, KIRP, LIHC, LUAD, LUSC, TGCT, and UVM (Fig. 3C). The UALCAN online tool confirmed that PFKP protein levels were significantly upregulated in RCC, HNSCC, LUAD, PAAC, and GBM (Fig. 3D).
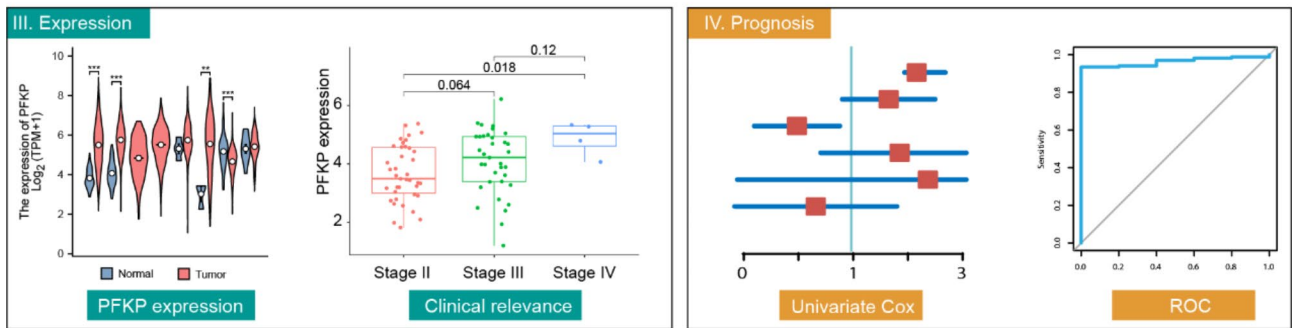
Correlation between PFKP expression and prognostic implications

The Kaplan-Meier analysis was used to evaluate the association between PFKP expression and OS, DSS, DFI, PFI in pan-cancer (Supplementary Figs. 1–4). Additionally, we further compared the survival contribution of PFKP in multiple cancer types, estimated using univariate Cox regression analyses (Fig. 4A–D). For example, the results showed that high PFKP as a risk factor for OS in ACC, CESC, HNSC, LAML, LIHC, LUAD, MESO, and UVM. Results for DSS, DFI, and PFI are shown in Fig. 4B–D. It is worth noting that PFKP was significantly associated with the survival of LUAD (all $P < 0.05$). These results suggested that PFKP expression had a strong prognostic power in different tumors, and the relevance of PFKP to clinical relevance may shed new light on the underlying pathogenesis of tumors.
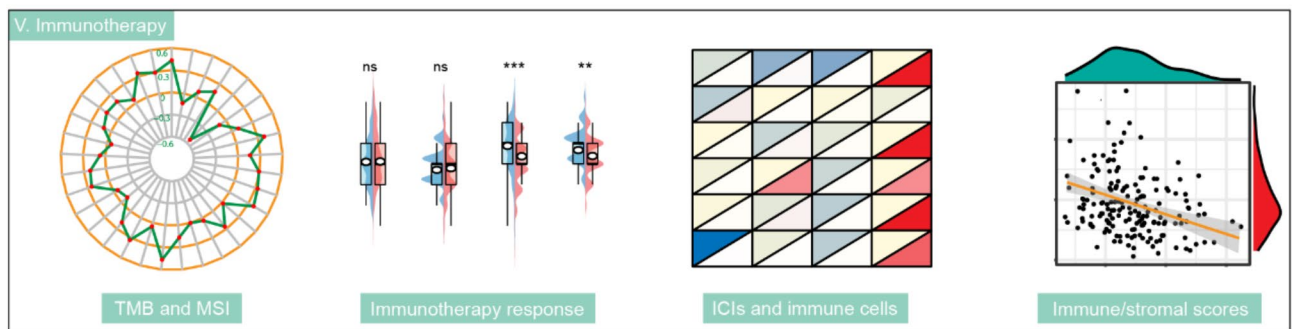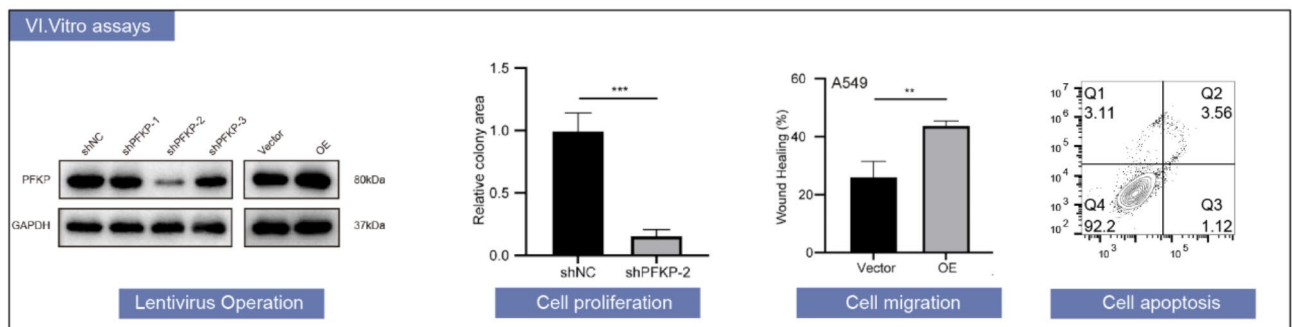
Fig. 1 The flow chart of our study

Ling *et al. Cancer Cell International*   (2024) 24:310

Page 6 of 15
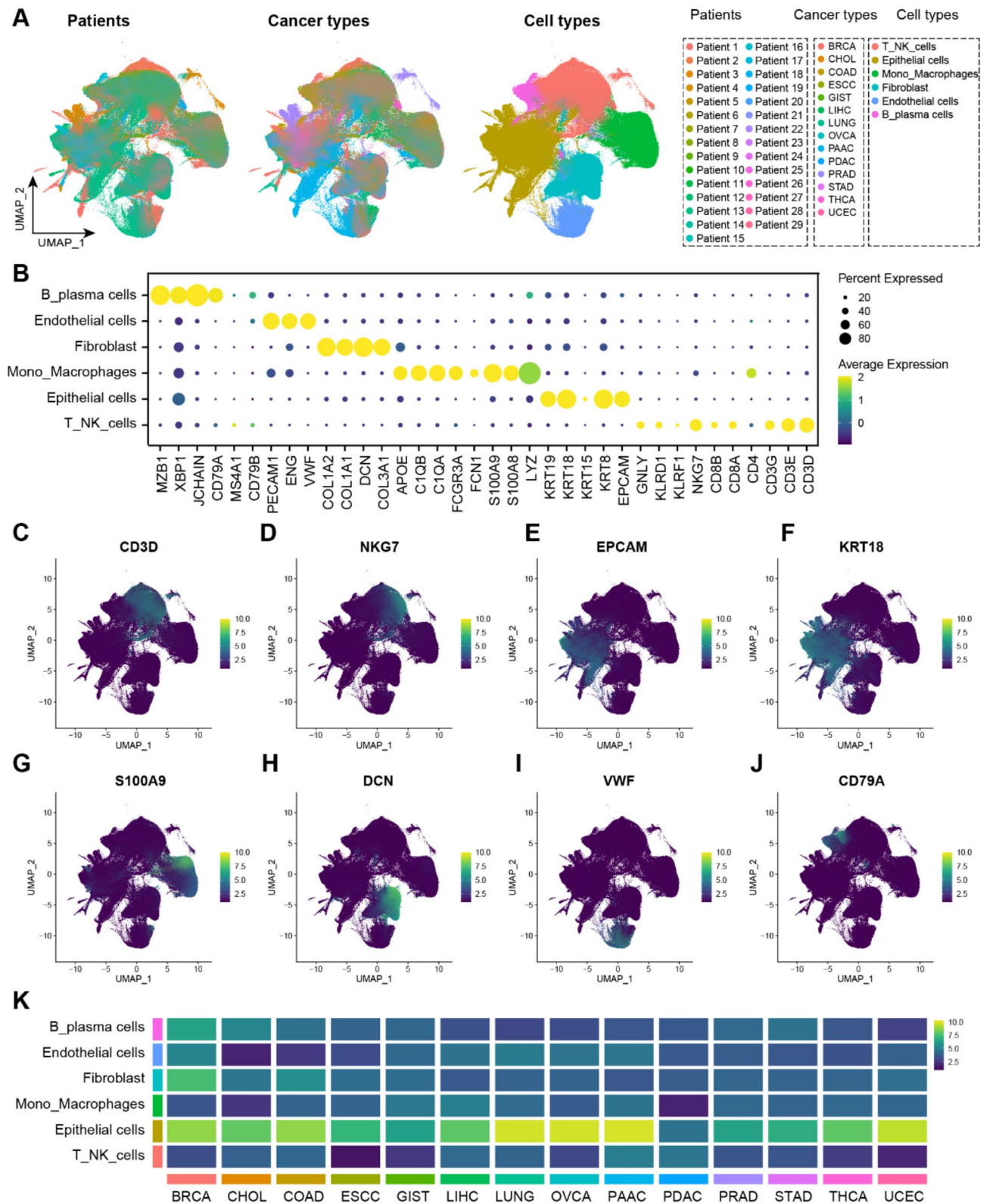
**Fig. 2** Pan-cancer single-cell transcriptome analysis of PFKP. (**A**). The UMAP plots showing the patients, cancer types and identified cell types. (**B**). Bubble diagram of cellular subpopulation marker genes. (**C**-**J**). The UMAP expression map of cellular subpopulation marker genes (**K**). Heatmap of PFKP expression in various cell populations in pan-cancer single cell data
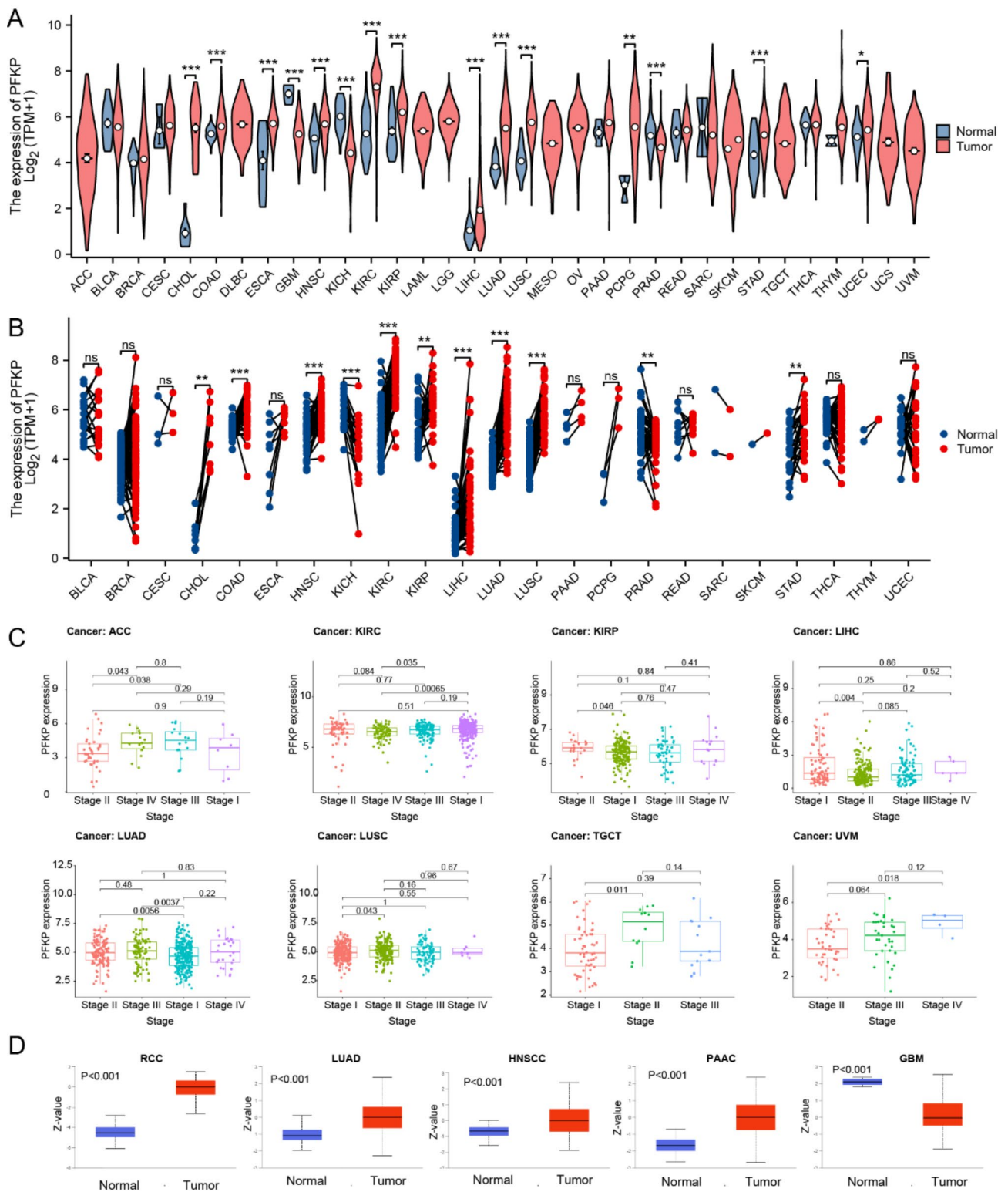
Fig. 3 The expression of PFKP in pan-cancer. (**A**). Differential expression of PFKP in normal and tumor samples of 33 tumors in TCGA database. (**B**). The differential expression of PFKP in paired samples. (**C**). Expression of PFKP in different pathological stages of indicated tumors. (**D**). PFKP protein expression levels between cancers and normal tissues. * $P < 0.05$, ** $P < 0.01$, and *** $P < 0.001$
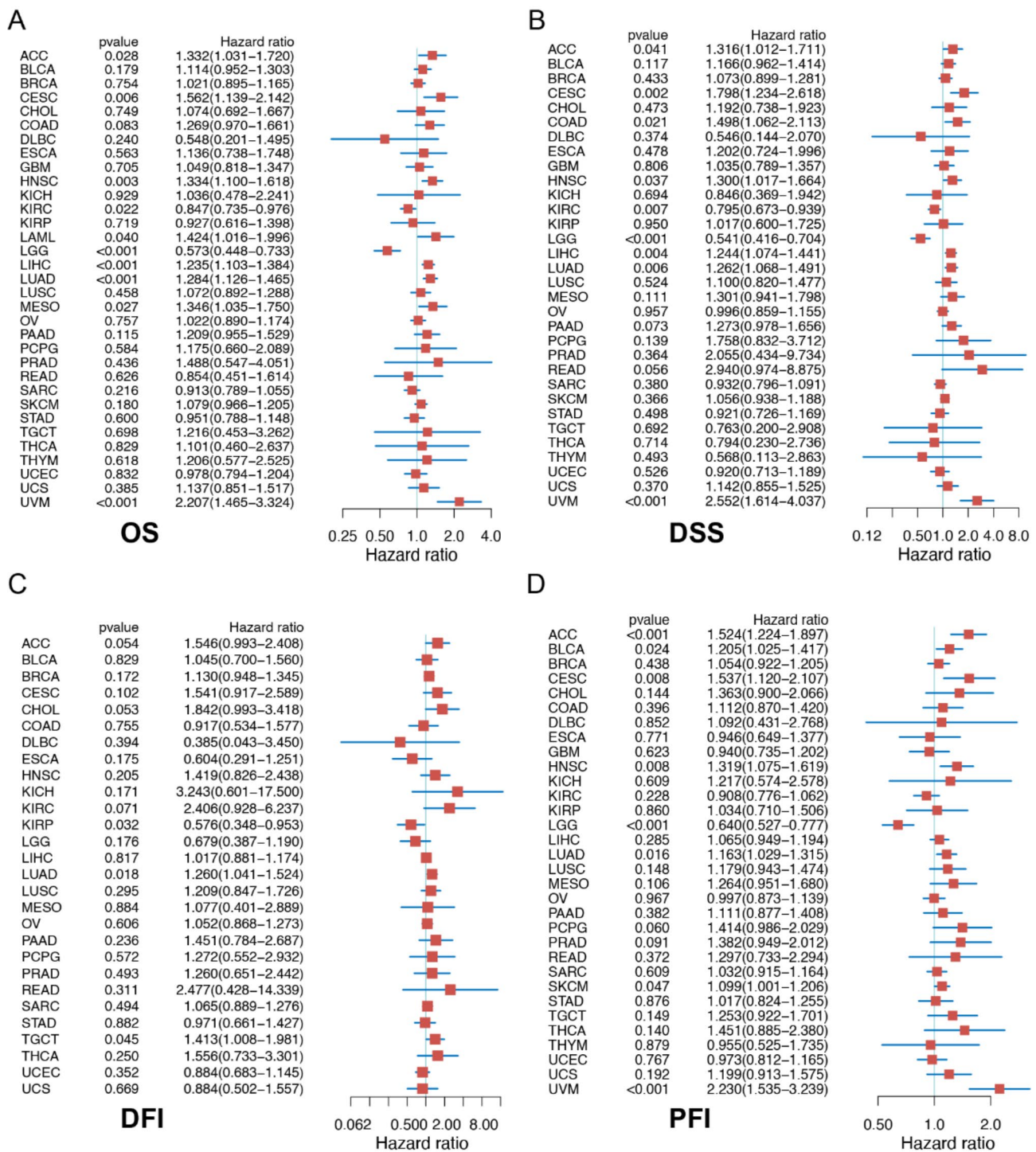
Fig. 4 Prognostic Potential of PFKP in Pan-Cancer. (**A**–**D**). The forest plots of univariate Cox regression analysis for OS (**A**), DSS (**B**), DFI (**C**), and PFI (**D**)

Diagnostic value of PFKP for pan-cancer

Given the significant differences in the expression levels of PFKP in different tumor tissues and corresponding normal tissues, we used the receiver operating characteristic (ROC) curve to initially investigate the diagnostic value of PFKP mRNA expression levels for discriminating between tumor and normal tissues (Fig. 5). The area under curve (AUC) values suggested that PFKP had a strong ability to discriminate, especially UCEC (AUC=0.665), THCA (AUC=0.605), PAAD (AUC=0.730), PCPG (AUC=0.927), PRAD (AUC=0.676), STAD (AUC=0.686), CESC (AUC=0.642), KIRP (AUC=0.803),
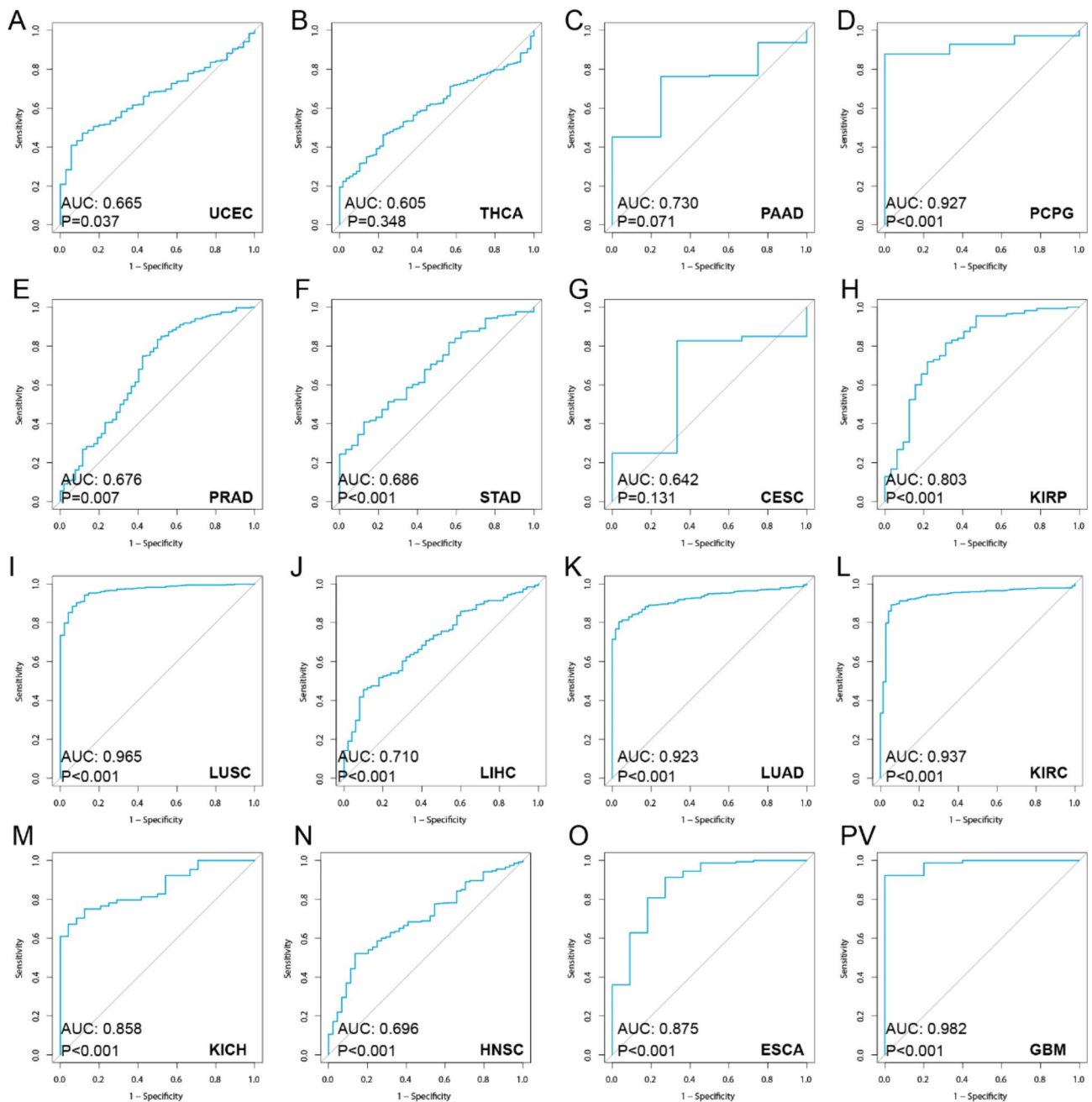
Fig. 5 Accuracy of PFKP in discriminating tumor from normal tissue in pan-cancer

LUSC (AUC=0.965), LUAD (AUC=0.923), LIHC (AUC=0.710), KIRC (AUC=0.937), KICH (AUC=0.858), HNSC (AUC=0.696), ESCA (AUC=0.875), and GBM (AUC=0.982). It can be seen that the PFKP mRNA expression level has a high diagnostic value for distinguishing tumors from normal tissues.

Association of PFKP expression with microsatellite instability, tumor mutation burden, and immunophenotype scores

Both microsatellite instability (MSI) and tumor mutation burden (TMB) are pivotal characteristics of tumors, and affect response to immunotherapy in cancers [23, 24], we next performed association analyses of PFKP expression with MSI and TMB. As shown in Fig. 6A, PFKP expression was positively correlated with MSI in BRCA, COAD, LGG, LUSC, STAD, and THYM, while negatively correlated with MSI in DLBC (all *P*<0.05). PFKP expression
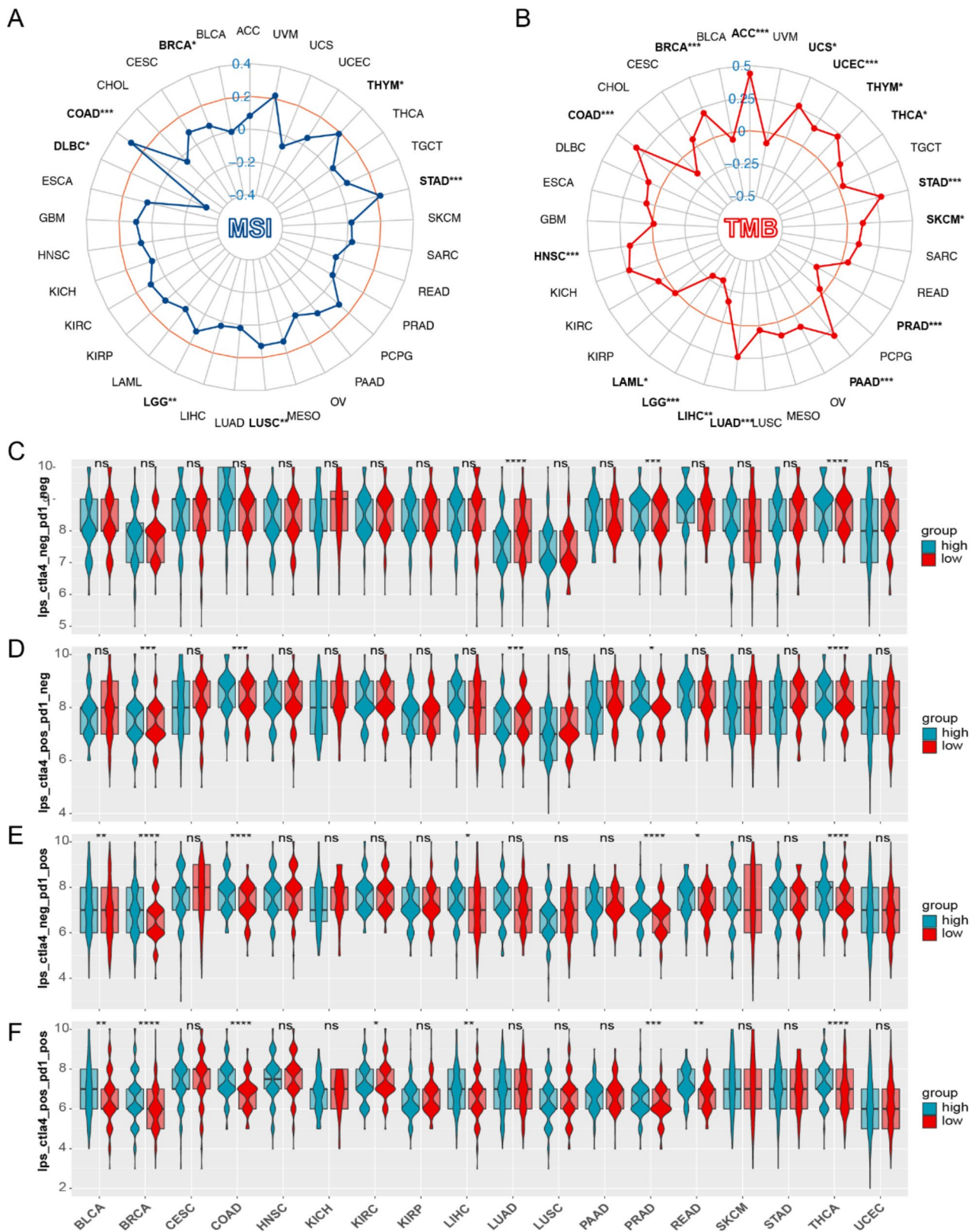
Fig. 6 Correlation between the expression of PFKP with MSI, TMB, and immune infiltration in pan-cancer. (**A**-**B**). Radar maps of correlations between PFKP expression and MSI (**A**) or TMB (**B**). (**C**-**F**). The difference of IPS between PFKP^high and PFKP^low expression groups. * $P < 0.05$, ** $P < 0.01$, and *** $P < 0.001$

was also positively correlated with TMB of ACC, BRCA, COAD, HNSC, LUAD, PAAD, SKCM, STAD, THCA, THYM, UCEC, and UCS, but negatively correlated with that of LAML, LGG, LIHC, and PRAD (all $P<0.05$) (Fig. 6B). Then, we used immunophenoscore (IPS) for LUAD patients from The Cancer Immunome Atlas to determine the sensitivity to immune checkpoint inhibitors for the PFKP (Fig. 6C-F). Our results showed that the high expression group possessed significantly higher immunophenotype scores (IPS) than the low expression group in PRAD and THCA. Moreover, the high expression group was more likely to gain benefits from anti-CTLA4 therapy in BRCA, COAD, PRAD, THCA, and respond to anti-PD1/PDL1/PDL2 therapies in BLCA, BRCA, COAD, LIHC, PRAD, READ, and THCA. Finally, the high expression group tended to respond to both anti-PD1/PDL1/PDL2 and anti-CTLA4 antibodies in BLCA, BRCA, COAD, LIHC, PRAD, READ, and THCA.

The association between PFKP and tumor immune microenvironment

Although our above investigations have demonstrated the prognostic ability of PFKP in pan-cancer, its potential role warranted further research. The development of malignant tumors is closely related to the tumor immune microenvironment (TIME) in which the tumor cells are located. TIME contains not only tumor cells but also immune cells, fibroblasts, and many other cells and extracellular matrix, which is the basis for the survival and development of tumor cells [25, 26]. It is unclear whether PFKP impacts the recruitment of immune cells. With several algorithms including EPIC, TIMER, QUAN-TISEQ, XCELL, MCP-counter, quanTIseq, CIBERSORT and CIBERSORT-ABS, we evaluated the correlation between the immune cell infiltration and PFKP expression in pan-cancer (Supplementary Figs. 5–7). Results indicated that PFKP was significantly associated with immune cell subsets in BRCA, HNSC, KIRC, LUAD, TGCT, and SKCM. In contrast, no correlation was found between PFKP expression and immune cell infiltration in ACC, CHOL, DLBC, KICH, MESO, and UCS. PFKP exhibited positive associations with dendritic cells, CD4^{+} T helper 2 cells, and negative associations with B cells, CD8^{+} T cells, native CD4^{+} T cells in the majority of tumors. Next, by adopting the ESTIMATE method, we computed the immune and stromal scores of cancer tissues. As Fig. 7 indicated, PFKP was positively correlated with the immune scores in BLCA, BRCA, COAD, LIHC, PRAD, and UVM, but negatively correlated with the immune score in ACC, CESC, GBM, HNSC, KIRP, LGG, LUSC, PAAD, TGCT, and THYM. For the analysis of the stromal score, we have obtained similar results (Supplementary Fig. 8).

### PFKP promoted proliferation and migration in LUAD cells

We then conducted in vitro experiments to validate the effects of PFKP. First, we assessed the expression levels of PFKP across different non-small cell lung cancer (NSCLC) cell lines (Fig. 8A). Based on the endogenous PFKP expression levels, we selected H1299 and A549 cells for PFKP gene knockdown and overexpression, respectively. Western blot analysis was performed to confirm the efficiency of these genetic manipulations (Fig. 8B). Silencing PFKP significantly reduced proliferation and colony formation in H1299 cells, whereas PFKP overexpression markedly enhanced proliferation in A549 cells (Fig. 8C-D). Additionally, we observed that PFKP knockdown inhibited migration in H1299 cells, while PFKP overexpression accelerated cell motility in A549 cells (Fig. 8E-F). Furthermore, PFKP knockdown significantly increased LDH release and apoptosis in H1299 cells, while PFKP overexpression suppressed LDH release and apoptosis in A549 cells (Fig. 8G-H).

Discussion

Our study has unveiled, for the first time, the critical role of PFKP in Pan-cancer. Through multidimensional analysis, we discovered that PFKP is consistently upregulated in the majority of tumors, with its expression increasing along with tumor stage in various cancers such as LUAD, LUSC, KIRC, HNSC, COAD, among others. Furthermore, high expression of PFKP is associated with poorer prognosis in most cancer patients. Negative correlations were observed between PFKP expression and overall survival rates in several tumors, including KICH, HNSC, LUAD, and others. Importantly, consistent results were obtained when analyzing different datasets, and published studies have also demonstrated the tumorigenic role of PFKP [7, 8, 27]. These findings suggest that PFKP possesses widespread oncogenic characteristics in cancer, holding significant prospects in the field of cancer research.

The tumor microenvironment (TME) is a highly structured ecosystem comprising various immune cells, cancer-associated fibroblasts (CAFs), endothelial cells (ECs), stromal cells, and other cell types, all embedded within a dynamic, vascularized extracellular matrix. These components are involved in intercellular communication, which can either promote or inhibit tumor progression [28, 29]. The TME plays a crucial role in determining the fate of tumor cells, not only by regulating their proliferation, invasion, and metastasis but also by influencing therapeutic outcomes [30]. Our findings indicate a correlation between the expression levels of PFKP and the TME across multiple cancer types. Consequently, we further investigated the relationship between PFKP and immunotherapy response. Microsatellite instability (MSI), tumor mutational burden (TMB), and the

Ling *et al. Cancer Cell International*   (2024) 24:310

Page 12 of 15
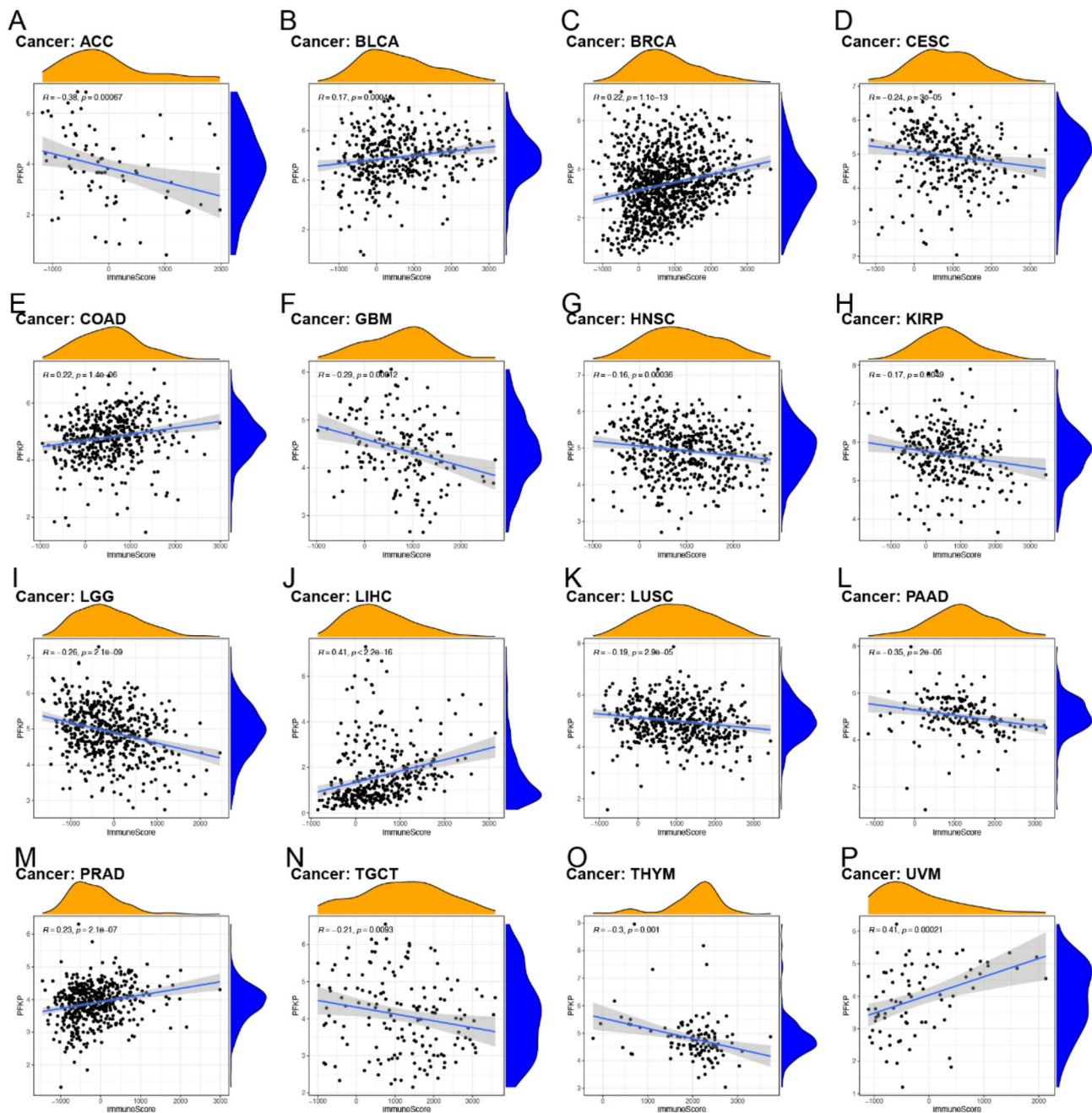
Fig. 7 Correlation between the expression of PFKP with immune scores in pan-cancer. (**A**-**P**). The scatter plots of correlation between PFKP expression and immune scores in multiple cancers. * $P < 0.05$, ** $P < 0.01$, and *** $P < 0.001$

expression levels of various immune checkpoint markers are closely associated with responses to immunotherapy and are important indicators for clinicians to identify patients who may benefit from such treatments [31]. Our analysis revealed a positive correlation between PFKP and MSI in six cancer types, including LUSC, BRCA, and COAD. Additionally, a significant correlation between PFKP and TMB was observed in 16 cancer types, including LUAD, BRCA, and HNSC. Furthermore, the

expression of PD-1 and CTLA-4 was also associated with PFKP across various cancers. In summary, this analysis employed clinically relevant indicators commonly used to assess the potential responsiveness of cancer patients to immunotherapy across 33 different tumor types, along with the corresponding targets of widely used immune checkpoint inhibitors. We did find correlations between PFKP and some cancers, though not all tumors showed a direct relationship with these indicators. However, it is
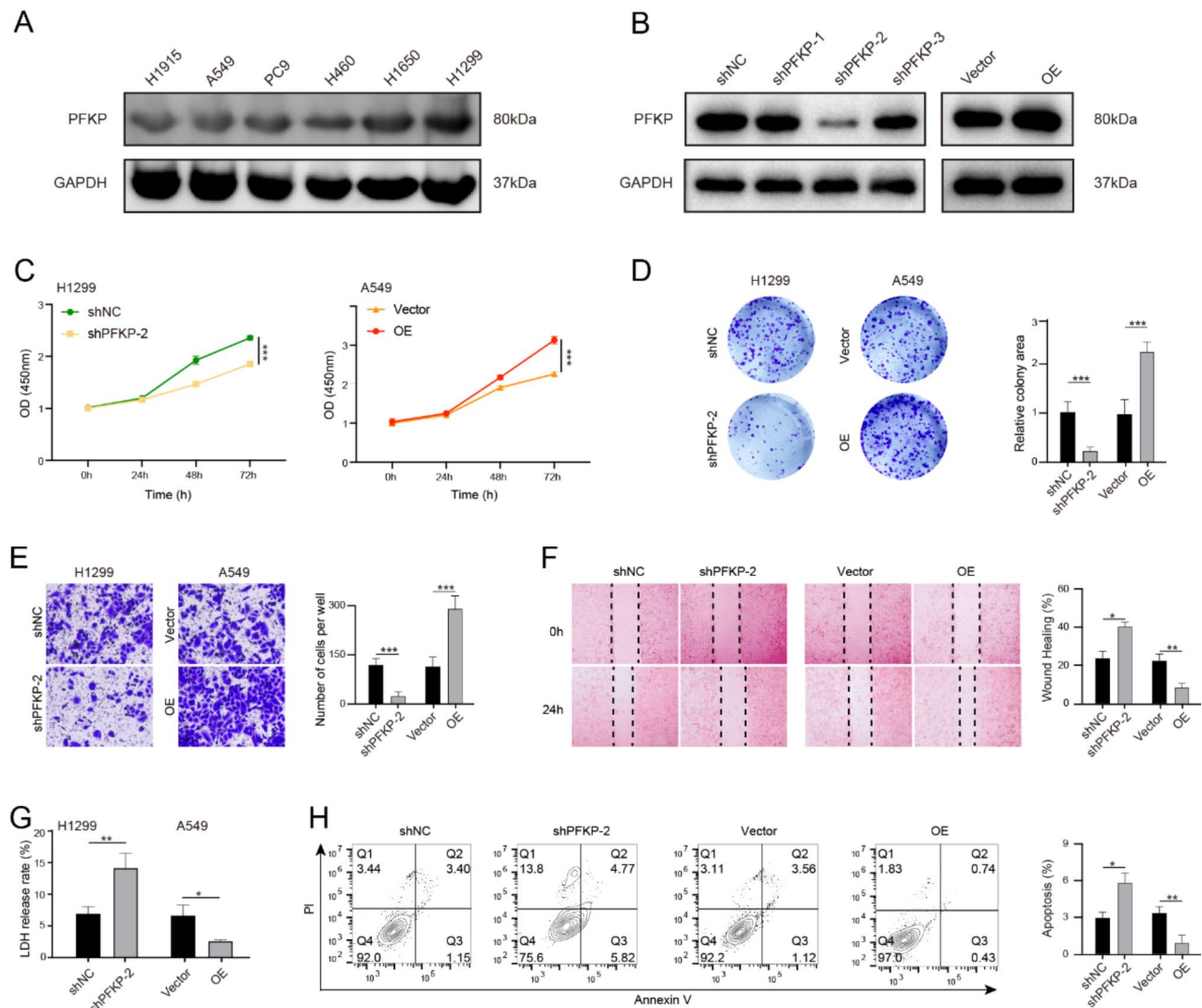
Fig. 8 The function of PFKP in lung cancer cells. (**A**). Differential expression of PFKP in lung cancer cells. (**B**). Examination of PFKP expression in A549 and H1299 cells stably infected lentiviral vectors overexpressing PFKP and lentiviral vectors carrying shPFKP, respectively. (**C, D**). The effects of overexpression or knockdown of PFKP on cell proliferation were verified by CCK-8 assay (**C**) and clone formation assay (**D**). (**E, F**). Transwell assay (**E**) and wound healing assay (**F**) verified the effect of overexpression or knockdown of PFKP on cell migration. (**G, H**). LDH release assay (**G**) and flow cytometry (**H**) were used to verify the effect of overexpression or knockdown of PFKP on cell apoptosis. * $P < 0.01$, ** $P < 0.01$, and *** $P < 0.001$

important to note that the regulation of gene sensitivity to immunotherapy varies significantly across different tumor types, reflecting the complexity of the TME and the diversity of gene regulatory mechanisms across cancers [32, 33]. These findings provide preliminary insights into the potential role of PFKP in various cancers and lay the groundwork for further research. Additionally, these comparisons help identify the unique behavior of this gene in specific cancers, which could inform future research on personalized immunotherapy strategies. Moreover, we focused on widely used clinical indicators for our correlation analysis. As cancer research progresses, more precise biomarkers may be developed in the future to better predict and enhance the effectiveness

of immunotherapy, thereby strengthening both clinical and basic research efforts.

Lastly, we validated the role of PFKP in lung cancer through in vitro experiments. Compared to normal bronchial epithelial cells, PFKP exhibited higher expression in lung cancer-associated tumor cell lines. Depletion of PFKP suppressed the proliferation and migration of H1299 cells. Conversely, overexpression of PFKP promoted the malignant phenotype of lung cancer cell lines.

Here, we have determined the crucial role of PFKP based on mining public databases and conducting in vitro experiments. With the release of a large volume of high-throughput data, researchers in this field have gained rich information and enlightening insights into

the understanding of the tumor microenvironment and the development of targets. However, it is important to note that results derived from public data and statistical algorithms may inevitably be influenced by significant heterogeneity and possible biases. The findings of bioinformatics analysis should be interpreted cautiously and cannot be directly translated into a clinical setting. In conclusion, we have identified PFKP as a potential biomarker for predicting different tumor prognoses and tumor immunogenicity, providing new avenues for the development of potential therapeutic targets in a clinical context.

Supplementary Information

The online version contains supplementary material available at https://doi.org/10.1186/s12935-024-03497-w.

Supplementary Material 1

Data availability
No datasets were generated or analysed during the current study.

Declarations

Ethical approval and consent to participate
Not applicable.

Consent for publication
Not applicable.

Competing interests
The authors declare no competing interests.

References
1. Remon J, Hendriks LEL, Mountzios G, Garcia-Campelo R, Saw SPL, Uprety D, Recondo G, Villacampa G, Reck M. MET alterations in NSCLC-Current perspectives and Future challenges. J Thorac Oncol. 2023;18(4):419–35.
2. Ozcan G, Singh M, Vredenburgh JJ. Leptomeningeal Metastasis from Non-small Cell Lung Cancer and Current Landscape of treatments. Clin Cancer Res. 2023;29(1):11–29.
3. Skok Z, Zidar N, Kikelj D, Ilas J. Dual inhibitors of human DNA topoisomerase II and other Cancer-related targets. J Med Chem. 2020;63(3):884–904.
4. Vora S, Miranda AF, Hernandez E, Francke U. Regional assignment of the human gene for platelet-type phosphofructokinase (PFKP) to chromosome 10p: novel use of polyspecific rodent antisera to localize human enzyme genes. Hum Genet. 1983;63(4):374–9.
5. Lang L, Chemmalakuzhy R, Shay C, Teng Y. PFKP Signaling at a glance: an emerging mediator of Cancer Cell Metabolism. Adv Exp Med Biol. 2019;1134:243–58.
6. Mulukutla BC, Yongky A, Daoutidis P, Hu WS. Bistability in glycolysis pathway as a physiological switch in energy metabolism. PLoS ONE. 2014;9(6):e98756.
7. Chen J, Zou L, Lu G, Grinchuk O, Fang L, Ong DST, Taneja R, Ong CN, Shen HM. PFKP alleviates glucose starvation-induced metabolic stress in lung cancer cells via AMPK-ACC2 dependent fatty acid oxidation. Cell Discov. 2022;8(1):52.
8. Peng M, Yang D, Hou Y, Liu S, Zhao M, Qin Y, Chen R, Teng Y, Liu M. Intracellular citrate accumulation by oxidized ATM-mediated metabolism reprogramming via PFKP and CS enhances hypoxic breast cancer cell invasion and metastasis. Cell Death Dis. 2019;10(3):228.
9. Tang Z, Li C, Kang B, Gao G, Li C, Zhang Z. GEPIA: a web server for cancer and normal gene expression profiling and interactive analyses. Nucleic Acids Res. 2017;45(W1):W98–102.
10. Chandrashekar DS, Bashel B, Balasubramanya SAH, Creighton CJ, Ponce-Rodriguez I, Chakravarthi B, Varambally S. UALCAN: a portal for facilitating Tumor Subgroup Gene expression and survival analyses. Neoplasia. 2017;19(8):649–58.
11. Zhu ZY, Tang N, Wang MF, Zhou JC, Wang JL, Ren HZ, Shi XL. Comprehensive Pan-cancer genomic analysis reveals PHF19 as a carcinogenic Indicator Related to Immune Infiltration and Prognosis of Hepatocellular Carcinoma. Front Immunol. 2021;12:781087.
12. Vega DM, Yee LM, McShane LM, Williams PM, Chen L, Vilimas T, Fabrizio D, Funari V, Newberg J, Bruce LK, et al. Aligning tumor mutational burden (TMB) quantification across diagnostic platforms: phase II of the friends of Cancer Research TMB Harmonization Project. Ann Oncol. 2021;32(12):1626–36.
13. Wu W, Liu Y, Zeng S, Han Y, Shen H. Intratumor heterogeneity: the hidden barrier to immunotherapy against MSI tumors from the perspective of IFN-gamma signaling and tumor-infiltrating lymphocytes. J Hematol Oncol. 2021;14(1):160.
14. Charoentong P, Finotello F, Angelova M, Mayer C, Efremova M, Rieder D, Hackl H, Trajanoski Z. Pan-cancer immunogenomic analyses reveal genotype-immunophenotype relationships and predictors of response to checkpoint blockade. Cell Rep. 2017;18(1):248–62.
15. Li B, Severson E, Pignon JC, Zhao H, Li T, Novak J, Jiang P, Shen H, Aster JC, Rodig S, et al. Comprehensive analyses of tumor immunity: implications for cancer immunotherapy. Genome Biol. 2016;17(1):174.
16. Aran D, Hu Z, Butte AJ. xCell: digitally portraying the tissue cellular heterogeneity landscape. Genome Biol. 2017;18(1):220.
17. Racle J, de Jonge K, Baumgaertner P, Speiser DE, Gfeller D. Simultaneous enumeration of cancer and immune cell types from bulk tumor gene expression data. Elife 2017, 6.
18. Finotello F, Mayer C, Plattner C, Laschober G, Rieder D, Hackl H, Krogsdam A, Loncova Z, Posch W, Wilflingseder D, et al. Molecular and pharmacological modulators of the tumor immune contexture revealed by deconvolution of RNA-seq data. Genome Med. 2019;11(1):34.
19. Newman AM, Liu CL, Green MR, Gentles AJ, Feng W, Xu Y, Hoang CD, Diehn M, Alizadeh AA. Robust enumeration of cell subsets from tissue expression profiles. Nat Methods. 2015;12(5):453–7.
20. Petitprez F, Levy S, Sun CM, Meylan M, Linhard C, Becht E, Elarouci N, Tavel D, Roumenina LT, Ayadi M, et al. The murine Microenvironment Cell Population counter method to estimate abundance of tissue-infiltrating immune and stromal cell populations in murine samples using gene expression. Genome Med. 2020;12(1):86.
21. Yoshihara K, Shahmoradgoli M, Martinez E, Vegesna R, Kim H, Torres-Garcia W, Trevino V, Shen H, Laird PW, Levine DA, et al. Inferring tumour purity and stromal and immune cell admixture from expression data. Nat Commun. 2013;4:2612.
22. Hao Y, Hao S, Andersen-Nissen E, Mauck WM 3rd, Zheng S, Butler A, Lee MJ, Wilk AJ, Darby C, Zager M, et al. Integrated analysis of multimodal single-cell data. Cell. 2021;184(13):3573–e35873529.
23. Aleksakhina SN, Imyanitov EN. Cancer Therapy guided by mutation tests: current status and perspectives. Int J Mol Sci 2021, 22(20).
24. Joshi SS, Badgwell BD. Current treatment and recent progress in gastric cancer. CA Cancer J Clin. 2021;71(3):264–79.
25. Xu L, Zou C, Zhang S, Chu TSM, Zhang Y, Chen W, Zhao C, Yang L, Xu Z, Dong S, et al. Reshaping the systemic tumor immune environment (STIE) and tumor immune microenvironment (TIME) to enhance immunotherapy efficacy in solid tumors. J Hematol Oncol. 2022;15(1):87.

26. Mao X, Xu J, Wang W, Liang C, Hua J, Liu J, Zhang B, Meng Q, Yu X, Shi S. Crosstalk between cancer-associated fibroblasts and immune cells in the tumor microenvironment: new findings and future perspectives. Mol Cancer. 2021;20(1):131.
27. Sha X, Wang K, Wang F, Zhang C, Yang L, Zhu X. Silencing PFKP restrains the stemness of hepatocellular carcinoma cells. Exp Cell Res. 2021;407(1):112789.
28. Bilotta MT, Antignani A, Fitzgerald DJ. Managing the TME to improve the efficacy of cancer therapy. Front Immunol. 2022;13:954992.
29. Chen D, Zhang X, Li Z, Zhu B. Metabolic regulatory crosstalk between tumor microenvironment and tumor-associated macrophages. Theranostics. 2021;11(3):1016–30.
30. Gao W, Wang X, Zhou Y, Wang X, Yu Y. Autophagy, ferroptosis, pyroptosis, and necroptosis in tumor immunotherapy. Signal Transduct Target Ther. 2022;7(1):196.
31. Yuan Z, Li Y, Zhang S, Wang X, Dou H, Yu X, Zhang Z, Yang S, Xiao M. Extracellular matrix remodeling in tumor progression and immune escape: from mechanisms to treatments. Mol Cancer. 2023;22(1):48.
32. Dong M, Yu T, Zhang Z, Zhang J, Wang R, Tse G, Liu T, Zhong L. ICIs-Related cardiotoxicity in different types of Cancer. J Cardiovasc Dev Dis 2022, 9(7).
33. Addeo A, Friedlaender A, Banna GL, Weiss GJ. TMB or not TMB as a biomarker: that is the question. Crit Rev Oncol Hematol. 2021;163:103374.
34. Roudko V, Cimen Bozkus C, Greenbaum B, Lucas A, Samstein R, Bhardwaj N. Lynch Syndrome and MSI-H cancers: from mechanisms to off-the-Shelf Cancer vaccines. Front Immunol. 2021;12:757804.

Publisher's note